arthropoda

MDPI

Article

Using Spectral Indices Derived from Remote Sensing Imagery to Represent Arthropod Biodiversity Gradients in a European *Sphagnum* Peat Bog

Maria A. Minor [1,*], Sergey G. Ermilov [2], Omid Joharchi [2] and Dmitriy A. Philippov [3]

[1] School of Natural Sciences, Massey University, Palmerston North 4410, New Zealand
[2] Tyumen State University, 625003 Tyumen, Russia
[3] Papanin Institute for Biology of Inland Waters, Russian Academy of Sciences, 152742 Borok, Russia
* Correspondence: m.a.minor@massey.ac.nz

Abstract: Monitoring of peatlands is an important conservation issue. We investigated communities of soil mites (Acari: Oribatida, Mesostigmata) inhabiting a relatively undisturbed European boreal mire characterized by a mosaic of oligotrophic and meso-eutrophic areas. We assess the potential of using remote sensing approach as a mapping and predictive tool for monitoring productivity and arthropod biodiversity in a peat bog. In georeferenced plots, Acari biodiversity, water table level, water pH and plot productivity class on the oligotrophic-eutrophic gradient were recorded. Data from the Landsat 8 OLI sensor were used to calculate several spectral indices known to represent productivity and surface moisture gradients in terrestrial ecosystems. We then explored the relationship between spectral indices, environmental gradients and biodiversity of mites. We found that several spectral indices were significantly and consistently correlated with local environmental variables and biodiversity of soil mites. The Excess Green Index performed best as a predictor of plot trophic class on the oligotrophic-eutrophic gradient and showed significant relationship with Oribatida diversity in 2016. However, following hot summer in 2019, there was no significant relationship between abundance and species richness of Oribatida and remotely sensed data; there was a weak correlation between abundance of Mesostigmata and spectral indices which represent surface moisture gradient (e.g., Normalised Difference Moisture Index). We discuss advantages and challenges of using spectral indices derived from remote sensing imagery to map biodiversity gradients in a peatland.

Keywords: peatlands; fauna; biodiversity; oribatid mites; Mesostigmata; remote sensing; Landsat 8 OLI; productivity

Citation: Minor, M.A.; Ermilov, S.G.; Joharchi, O.; Philippov, D.A. Using Spectral Indices Derived from Remote Sensing Imagery to Represent Arthropod Biodiversity Gradients in a European *Sphagnum* Peat Bog. *Arthropoda* **2023**, *1*, 35–46. https://doi.org/10.3390/arthropoda1010006

Academic Editor: José Max Barbosa Oliveira Júnior

Received: 15 November 2022
Revised: 14 December 2022
Accepted: 20 December 2022
Published: 31 December 2022

1. Introduction

Ombrotrophic (rain-fed) peat bogs are characterized by high water table, acidic nutrient-poor conditions and dominance of *Sphagnum* mosses and occur in the boreal and temperate zone on most continents [1]. Worldwide, peatland environments are important as providers of ecosystem services and as long-term carbon storage reservoirs [2–4].

The plant communities of peat bogs provide information on ecosystem processes such as primary production and carbon sequestration and are sensitive indicators of environmental change [5–11]. Based on plant communities, bog environments are usually classified along the oligotrophy–eutrophy 'productivity' gradient [12]. Although not strictly a nutrient gradient, as plant communities reflect predominantly the gradient of pH values, the oligotrophy–eutrophy gradient frequently also reflects the availability of nutrients [13,14]. If a bog receives an additional nutrient input, either globally in the form of nutrient pollution from atmospheric sources, or locally from mineral-rich ground water seepage or from surface streams, the resulting areas of nutrient enrichment are characterized by higher pH and characteristic changes in vegetation [15]. The second major gradient in bogs is the ground water level, driven by the micro-topography of hummocks and hollows, which

gives bogs their characteristic patterning and which is linked to hydrology and carbon sequestration [1,16]. Both productivity and microtopography exert significant controls on patterns of plant and animal diversity in peat bogs.

Bog environments are a habitat for many species; among invertebrates which are abundant in peat bogs are mites (Arthropoda: Acari). Mite taxa such as Oribatida are well studied, abundant and diverse, and are known to respond to a wide range of environmental and anthropogenic stressors in bogs and elsewhere [17–25]. At a site level, the diversity patterns of mites are influenced by the same gradients that are recognized as richness drivers for broader groups of bog organisms, such as pH, nutrient availability and ground water level [25,26].

Peat bogs worldwide have been affected by nutrient pollution, peat extraction, drainage and other types of development, leading to degradation and loss of biological diversity [2,3,27]. Consequently, monitoring of environmental conditions and productivity of peatlands is important. Due to access difficulties and expense of ground sampling in remote peat bogs, coupled with the need for spatially-explicit landscape-scale information, various remote sensing methods have been used for monitoring of peatlands [28–32]. For example, remote sensing has been used to obtain information on bog hydrology and water table depth, functional types and phenology of plants, and to map vegetation classes and fertility gradients [9,28,29,31,33,34]. Other relevant values, such as the Leaf Area Index or the Normalized Difference Vegetation Index, both important parameters linked to terrestrial ecosystem productivity, are routinely mapped using spectral indices derived from remote sensing imagery [10,35–39].

Because satellite data can be remotely obtained and are free for satellites such as Landsat 8 or Sentinel-2, they are useful to enhance our understanding of response of bog arthropod communities to productivity gradients in less accessible areas. In this study, we investigated communities of free-living mites inhabiting a relatively undisturbed European boreal mire "Shichengskoe". Shichengskoe mire system is characterized by a mosaic of oligotrophic and meso-eutrophic areas, and our previous data for this system show that the pH gradient and the nutrient availability gradient in this bog are linked [25]. The trophic class of sampled plots (classified on a oligotrophy–eutrophy gradient based on plant community features) was one of the best predictors of abundance and species richness of non-aquatic oribatid mites in this bog [25]. For aquatic Oribatida, water table depth was of significant importance [25]. Mesostigmatid mites of the bog have not been studied previously. Here, we aimed to assess the potential of using remote sensing data as a mapping and predictive tool for monitoring arthropod biodiversity of a peat bog. As the connection between environmental data and mite biodiversity can been demonstrated directly, we aimed to confirm the link between spectral data and environmental data and to check if the link between spectral data and biodiversity data is consistent with the ground survey results.

2. Materials and Methods

2.1. Study Site

The mire system "Boloto Shichengskoe" in Vologda region in the north-western Russia (59°56′30.4″ N, 41°16′57.1″ E, 120 m a.s.l.) is a large (15,900 ha) wetland system of predominantly lacustrine origin (Figure 1a). The central part of the mire is occupied by a shallow oligotrophic lake Shichengskoe (1060 ha). Extensive area of the mire is the oligotrophic peat bog, dominated by *Sphagnum* mosses. Within the oligotrophic bog, there are several ground water seeps, associated with forested (*Picea*-*Pinus*-shrublets) islands. Areas near the seeps and the south-eastern part of the mire system are meso- and eutrophic [40]. The climate in the region is humid continental (Dfb in Köppen climate classification) with long moderately cold winter (mean temperature of January −12 °C) and short warm summer (mean temperature of July 16–17 °C). Annual precipitation is 500–650 mm; snow cover lasts 165–170 days of the year [40].

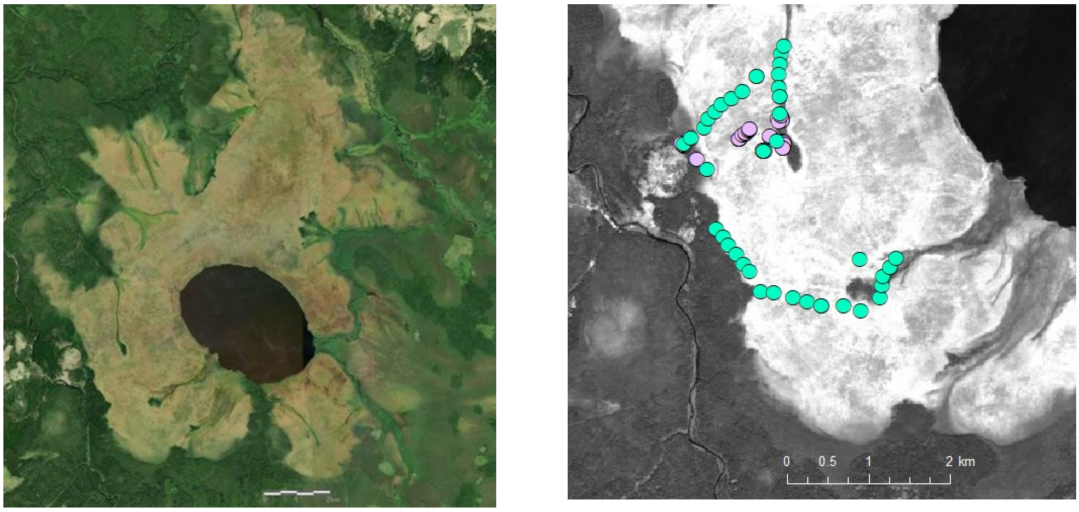

(**a**) (**b**)

Figure 1. Study area: (**a**) Shichengskoe mire system with Shichengskoe lake (scale bar: 2 km); in lighter colour is the ombrotrophic *Sphagnum* peat bog. Image courtesy of the U.S. Geological Survey. (**b**) Sampling plots, 2016—purple, 2019—green (scale bar: 2 km).

2.2. Sampling on the Ground

Two ground datasets were used in this study. The first dataset (training set) was collected in July 2016 in *Sphagnum*-dominated communities in the ombrotrophic western part of the mire system (Figure 1b). Samples were collected from 48 plots dominated by *Sphagnum* species; each plot was 1 m^2 in size. The minimum distance between plots was 5–7 m, but usually over 30 m. In each sampling plot, the following was recorded: GPS coordinates, *Sphagnum* moss identity, water table level, water pH and *Sphagnum* nutrient content (C, N, P, K) (see details in [25]). Based on plant community features, each plot was assigned to one of the five qualitative productivity classes ("trophic classes") on the oligotrophic–eutrophic gradient (oligotrophic, oligo-mesotrophic, mesotrophic, meso-eutrophic, eutrophic) [41,42]. Such trophic classes do not directly reflect nutrient status, but instead are based on plant indicator species of the poor-rich (acidity–alkalinity) gradient—however, in Shichengskoe mire these trophic classes are correlated with pH and *Sphagnum* nutrient content measurements [25]. The distribution of trophic classes among plots was not homogeneous, as meso-eutrophic and eutrophic patches are rarer on the ground. There were 21 oligotrophic plots, 18 oligo-mesotrophic and mesotrophic plots, and 9 meso-eutrophic and eutrophic plots. *Sphagnum* moss for mite extraction was collected as 10 × 10 cm samples to the depth of living moss plants (including capitula and the length of stems) (one sample per plot). Mites from moss samples were extracted in modified Berlese funnels until samples were fully dry (at least for five days). Adult Oribatida were identified to a species level using published keys and original species descriptions and classified into two functional groups following [22,43]—'aquatic' species, living on submerged vegetation in freshwater habitats, and 'terrestrial' (all other species). Oribatida juveniles were excluded from abundance and richness counts.

The second dataset (validation set) was collected in August 2019 using the same methods, except *Sphagnum* nutrient content was not measured. Sampling was again limited to 1 m^2 plots in *Sphagnum*-dominated communities but covered a larger extent of the mire (Figure 1b). In each sampling plot GPS coordinates, *Sphagnum* moss identity, trophic class on the oligotrophic–eutrophic gradient, ground water level and pH were recorded. Mites were sampled and extracted using the same methods as above. Adult Oribatida and Mesostigmata were identified to a species level. Aquatic and terrestrial Oribatida were counted separately, with juveniles excluded. Mesostigmata are all terrestrial; their juveniles were excluded from abundance and richness counts. Some of the records in this dataset

were excluded from the analysis as plots were located too close to each other—at the end, the dataset comprised 42 records (see Data S1 in Supplementary Materials).

2.3. Remote Sensing Data

The U.S. Geological Survey Landsat 8 OLI/TIRS scenes for path 177, row 18 covering Vologda region were used with the 2016 (scene LC81770182016151LGN01, 30 May 2016) and 2019 (scene LC08_L2SP_177018_20190608_20200828_02_T1, 6 August 2019) data sets. The satellite imagery search criteria were (a) acquisition date close to the date of sampling and the period of maximum vegetation activity and (b) minimum cloud cover (5% threshold). The 24-Jul-2016 scene, also available, was rejected due to the larger % cloud cover and the presence of haze.

Remote sensing images require radiometric and geometric correction. The path 177 row 18 scenes for 30 May 2016 and 6 August 2019 are "level T1", indicating that they have been geometrically corrected. As a rule, systematically corrected T1 Landsat 8 data have geodetic accuracy of $\leq$12 m [44].

The remote sensing data were processed using the ArcMap 10.6, Esri Inc., Redlands, CA, USA. Landsat 8 scenes were cropped to the area of interest and co-registered. The 16-bit digital numbers (DN_{band}) recorded in the Landsat 8 OLI spectral radiance bands 2–7 were converted to the top of the atmosphere band reflectances (r_{band}) using solar zenith angle and band-specific scaling coefficients provided in the Landsat 8 OLI metadata file [44]. Spectral bands were significantly correlated to local environmental data (Table 1). However, such correlations are difficult to interpret biologically, so we focused on known spectral indices which represent productivity gradients and surface moisture gradients in terrestrial ecosystems.

Table 1. Landsat 8 OLI (path 177, row 18, 30-May-2016) bands correlations with water pH, plot trophic class and water table depth in Shichengskoe mire (Pearson r, * $p < 0.05$, ** $p < 0.01$).

	Band 2	Band 3	Band 4	Band 5	Band 6	Band 7
pH	−0.17	−0.06	−0.15	0.09	−0.22	−0.45 **
Trophic class	−0.32 *	−0.13	−0.38 **	−0.11	−0.22	−0.46 **
Water table depth	0.30 *	0.26	0.35 *	0.38 **	0.19	0.09

The following spectral indices representing productivity gradient and ground water level gradient were calculated for the area of interest and sampled using ground plot coordinates:

(i) Normalized Difference Vegetation Index (NDVI), computed using band 4 (red) and band 5 (NIR) reflectances as (r5 − r4)/(r5 + r4). NDVI is an indicator of the amount of vegetation; it approaches 1.0 if a pixel contains vegetation; 0 if a pixel contains soil; and −1.0 if a pixel contains water. NDVI is commonly used in remote sensing as a proxy for productivity [36];

(ii) Excess Green (ExG), calculated as 2r3 − r4 − r2;

(iii) Excess Green minus Excess Red (ExG−ExR), calculated as 1.4r4 − r3 using normalized reflectances of band 2 (blue), band 3 (green) and band 4 (red) [45]. Both ExG and ExG−ExR have been found useful as proxies of gross primary productivity [45,46];

(iv) Normalized Difference Moisture Index (NDMI), computed using band 5 (NIR) and band 6 (SWIR1) reflectances as (r5 − r6)/(r5 + r6) [47]. NDMI is used to determine vegetation water content; it is sensitive to changes in liquid water content and in spongy mesophyll of vegetation canopies [47,48], otherwise known as NDWI (normalized difference water index);

(v) Moisture Stress Index (SWIR1/NIR), computed as r6/r5; this index is negatively correlated with surface water content and has been suggested as a broad-band index of surface moisture (reflective of water table position) in peatlands [32,49]. Moisture

Stress Index is used for canopy stress analysis, productivity prediction and biophysical modeling [50].

2.4. Data Analysis

The values of spectral indices were calculated and extracted from the satellite imagery for the GPS coordinates of plots using the ArcMap 10.6 software package. The values of spectral indices were compared with local-scale environmental and biodiversity parameters for that year using Pearson correlation in R 4.0.5. Variables at a plot level in 2016 were: water table level; water pH; *Sphagnum* nutrient content (C, N, K, P); trophic class; Oribatida abundance and species richness (see [25] for detailed analysis of 2016 data). Variables at a plot level in 2019 were: water table level; water pH; trophic class; Oribatida abundance and species richness; Mesostigmata abundance and species richness.

The 2016 dataset was used as a training set—using the 2016 data, the spectral indices with the significant correlation to environmental and biodiversity parameters were selected to develop the regression model. Random forest regression (randomForest package in R) [51] was employed for variable selection and to predict the trophic class of ground plots. The output provides the total % variance explained, and the importance score for each explanatory variable. The significance of random forest model was tested using permutation procedure (rfUtilities package in R 4.0.5; [52]).

3. Results

Previous results showed that plot trophic class and water table depth were the two best predictors of Oribatida biodiversity in Shichengskoe mire [25]. Higher abundance and species richness of oribatid mites in 2016 were correlated with higher productivity and lower water table depth (Table 2). In 2019, we observed no relationship between plot trophic class and abundance, or species richness of mites (Table 2) and the total abundance of mites collected in 2019 sampling was low (Appendix A, Tables A1 and A2), possibly due to the heat wave anomaly—June and July 2019 were the hottest months on record for the region. The relationship between water table level and mite diversity, on the other hand, remained consistent between 2016 and 2019, with higher abundance and richness of terrestrial Oribatida and Mesostigmata associated with lower water table (Table 2).

Table 2. Pearson's correlations (*r*, + $p < 0.1$, * $p < 0.05$, ** $p < 0.01$, *** $p < 0.001$) for local environmental data and mite diversity in Shichengskoe mire; na—data not collected in 2016.

		Mesostigmata Diversity		**Oribatida Diversity**		
		Abundance	**Richness**	**Abundance, Aquatic**	**Abundance, Terrestrial**	**Richness, Terrestrial**
2019	Trophic class	−0.07	0.03	0.26 +	−0.09	−0.04
	pH	−0.10	−0.04	0.17	−0.08	−0.08
	Water table depth	−0.54 ***	−0.45 **	0.28 +	−0.21	−0.33 *
2016	Trophic class	na	na	−0.24	0.46 ***	0.63 ***
	pH	na	na	0.12	0.06	0.19
	Water table depth	na	na	0.66 ***	−0.44 **	−0.41 **

Landsat 8 OLI spectral indices representing productivity gradient and ground water level gradient were consistently correlated to local environmental gradients in Shichengskoe mire in both 2016 and 2019 data sets (Tables 3 and 4). ExG and NDVI performed well as productivity indices, showing significant correlative relationship with trophic classification of sampling plots. The NDMI and SWIR1/NIR showed significant correlation with water table depth in both data sets. ExG−ExR was correlated to both trophic class and ground water level in 2016, but only to trophic class in 2019.

Table 3. Pearson's correlations (r, + $p < 0.1$, * $p < 0.05$, ** $p < 0.01$, *** $p < 0.001$, $n = 48$) for Landsat 8 OLI spectral indices, local environmental data and Oribatida biodiversity in Shichengskoe mire (July 2016). NDVI—Normalized Difference Vegetation Index; ExG—Excess Green index; ExG−ExR—Excess Green minus Excess Red index; NDMI—Normalized Difference Moisture Index; SWIR1/NIR—Moisture Stress Index.

Index	Trophic Class	pH	Water Table Depth	Nutrients in *Sphagnum* Tissues			Oribatida Diversity		
				C:N	P	K	Abundance, Aquatic	Abundance, Terrestrial	Richness, Terrestrial
NDVI	0.55 ***	0.47 **	0.13	−0.19	−0.31 *	0.21	−0.18	0.38 **	0.45 ***
ExG	0.63 ***	0.25 +	−0.19	−0.24 +	−0.28 +	0.37 **	−0.35 **	0.52 ***	0.63 ***
ExG−ExR	−0.54 ***	−0.21	0.39 **	0.34 **	−0.43 **	−0.36 **	0.26 +	−0.41 **	−0.50 ***
NDMI	0.08	0.27 +	0.35 **	0.09	−0.60 ***	−0.05	0.06	0.00	0.02
SWIR1/NIR	−0.11	−0.27 +	−0.33 **	−0.08	0.61 ***	0.03	−0.04	−0.03	−0.06

Table 4. Pearson's correlations (r, + $p < 0.1$, * $p < 0.05$, ** $p < 0.01$, $n = 42$) for Landsat 8 OLI spectral indices, local environmental and productivity data, and mite biodiversity in Shichengskoe mire (August 2019).

Index	Trophic Class	pH	Water Table Depth	Mesostigmata Diversity		Oribatida Diversity		
				Abundance	Richness	Abundance, Aquatic	Abundance, Terrestrial	Richness, Terrestrial
NDVI	0.35 *	0.21	−0.15	0.26 +	0.19	0.20	0.01	−0.03
ExG	0.14	0.23	0.16	−0.09	0.11	−0.11	−0.02	−0.05
ExG−ExR	−0.44 **	−0.22	0.13	−0.25	−0.20	−0.20	−0.01	0.01
NDMI	−0.15	0.01	0.42 **	−0.30 +	−0.26 +	−0.12	−0.11	−0.12
SWIR1/NIR	0.15	0.00	−0.42 **	0.30 *	0.25	0.13	0.10	0.11

Spectral indices representing productivity gradient were significantly correlated with oribatid mites biodiversity in 2016, consistent with the ground data; the strongest relationship was between Oribatida biodiversity and the ExG index (Table 3, Figure 2a,b). However, spectral indices representing ground water level gradient showed no correlation with Oribatida diversity in 2016, even though the ground data (Table 2) suggest that this gradient was important. In the 2019 dataset, a significant correlation was seen between abundance and richness of Mesostigmata and spectral indices representing water table gradient, which is consistent with the ground data (Tables 2 and 4).

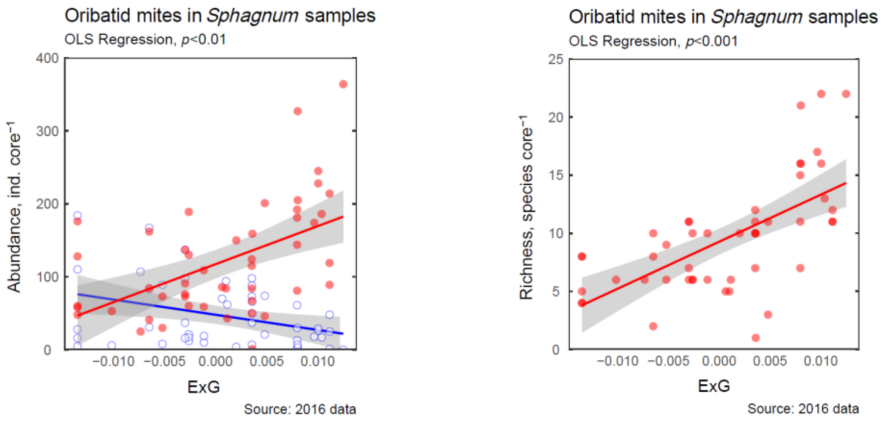

(**a**) (**b**)

Figure 2. Landsat 8 OLI spectral index ExG vs. biodiversity of oribatid mites in *Sphagnum* bog plots (red—terrestrial Oribatida, blue—aquatic Oribatida), Shichengskoe mire, July 2016: (**a**) abundance; (**b**) species richness.

Random forest regression model predicting trophic class using spectral indices was significant at $p < 0.001$, with ExG index again showing as the best predictor of trophic class

(Table 5). The random forest model based on 2016 satellite and ground data predicted the trophic class of plots visited in 2019 with 69.0% accuracy; this of course is relying on the assumption that the trophic class did not change between 2016 and 2019.

Table 5. Random forest model variable selection for Landsat 8 spectral indices best explaining plot trophic class (based on plant indicator species of the poor-rich (acidity–alkalinity) gradient) in Shichengskoe mire, July 2016. The higher % increase MSE, the more important a variable is in explaining observed patterns.

Model Information	Variable Selection	%IncMSE
No. of trees: 300		
No. of variables tried at each split: 3	ExG	0.375
Mean of squared residuals: 0.234	ExG−ExR	0.124
No. of permutations: 999	NDVI	0.047
Model significant at p = 0.001	SWIR1/NIR	0.027
Model R-square: 0.528	NDMI	0.023

4. Discussion

The use of data derived from remote sensing imagery for assessment and prediction of biodiversity is receiving increasing attention [53–56]. Unlike vegetation, soil communities cannot be directly linked to spectral indices, but close links between landscape forms, vegetation and soil biota allow us to link information from remote sensors to soil biodiversity patterns. There are only a few such studies—but, for example, satellite-derived spectral information has been used to predict patterns of biodiversity in soil microbiome communities, soil mesofauna (springtails) and earthworms [57–59].

Our results demonstrate both the potential and the limitations of using freely available satellite data for generating information on environmental gradients, productivity and biodiversity in a peatland. Among spectral productivity indices, the ExG index was the best predictor of trophic class and could be used as a broad-scale variable representing productivity gradient in the Shichengskoe mire, with a significant relationship with Oribatida diversity. Both ExG and ExG−ExR have been used successfully elsewhere as a proxy for gross primary productivity [45,46]. On the other hand, NDVI is known to perform less well in peatland environments due to atypical near-infrared reflectance of *Sphagnum* mosses [60,61].

The application of spectral indices derived from remote sensing imagery to map ecological gradients in peatlands presents several challenges. The first of these is the scale—for medium-scale sensors such as Landsat 8 OLI or Sentinel-2, it results in aggregation and averaging of patterns and features which are smaller than the pixel size of the sensor [28]. The use of fine-scale sensors such as IKONOS improves the accuracy of peatland land cover mapping [31] but is more costly. The second challenge is the difficulty of deriving the details of bog microtopography from the satellite sensor data. Peat bog microtopography (hummocks and hollows) are linked to hydrology and biodiversity [1,24,26]. In the Shichengskoe mire, two major environmental drivers which explained the abundance, species richness and community composition of Oribatida were trophic class, linked to acidity–alkalinity (pH) gradient and nutrients (N-P-K) availability, and water table level, linked to microtopography [25]. For aquatic Oribatida, the water table was the single most important variable [25]. Our 2019 data (this study) suggests again that microtopography and moisture are significant drivers for diversity of both Oribatida and Mesostigmata mites. A satellite sensor, by definition, records a "flat' pixel reflectance value and loses structural information, which may result in a poor discrimination of microtopography and its effects. Soil moisture indices (such as NDMI) may have limitations in peat bog environment, especially during dry conditions [32,62]. Crichton et al. [28] used Landsat ETM+ to map the spatial distribution of six ecohydrological classes on a lowland ombrotrophic peatland in the UK; their accuracy with Landsat ETM+ bands alone was 74%; including the texture brightness layer derived from band 5 increased accuracy of prediction.

Other option includes supplementing satellite imagery with airborne Light Detection and Ranging (LiDAR) data [31,63,64] or using the Synthetic Aperture Radar (SAR) backscatter in Sentinel-1 satellite [65], which adds information on surface texture and water table depth to increase accuracy.

5. Conclusions

To conclude, Landsat 8 OLI spectral indices representing productivity gradient and ground water level gradient were consistently correlated to local environmental gradients in Shichengskoe mire. Spectral indices were significantly correlated with mite biodiversity parameters, and the patterns were consistent with the ground data; the strongest relationship was between Oribatida biodiversity and the ExG index in 2016. Changing weather conditions can override local environmental gradients, as we have seen with lower abundance and diversity of Oribatida after the abnormally hot summer of 2019.

There is an opportunity to use freely available medium-scale remotely sensed data for soil biodiversity monitoring in space and time, once the links between biodiversity of specific taxa and land features which affect land reflectance values (e.g., soil type, soil moisture, vegetation) are established. Ground data should be used to validate the accuracy of predictions. Surface topography (e.g., digital elevation model) and texture (roughness, microtopography) data, if possible, should be used to supplement spectral data.

Supplementary Materials: The following supporting information can be downloaded at https://www.mdpi.com/article/10.3390/arthropoda1010006/s1, Data S1: Sampling plots in Shichengskoe mire: sampling dates, GPS coordinates, environmental parameters, dominant *Sphagnum* species.

Author Contributions: Conceptualization, M.A.M. and D.A.P.; methodology, D.A.P., S.G.E., O.J. and M.A.M.; fieldwork, D.A.P.; data analysis, S.G.E., O.J. and M.A.M.; writing—original draft preparation, M.A.M.; writing—review and editing, S.G.E. and D.A.P.; funding acquisition, D.A.P. and S.G.E. All authors have read and agreed to the published version of the manuscript.

Funding: This research was partially supported by the cooperative agreement No. FEWZ-2021-0004 from the Russian Ministry of Science and Higher Education. Work by D.A. Philippov was supported within the framework of the state assignments from the Ministry of Science and Higher Education of the Russian Federation (project no. 121051100099-5). Fieldwork was carried out as a part of the Russian Science Foundation grant no. 14-14-01134 and Russian Foundation for Basic Research grant no. 18-04-00988.

Data Availability Statement: The data on mite biodiversity presented in this study are available from the corresponding author upon request. Voucher specimens for identified species are in authors' own collection, S.E. (Oribatida) and O.J. (Mesostigmata), Tyumen State University, Tyumen, Russia. The Landsat 8 imagery is publicly available at https://www.usgs.gov/landsat-missions/landsat-data-access, accessed on 12 November 2022.

Acknowledgments: We thank Alexander A. Prokin (Papanin Institute for Biology of Inland Waters, Russian Academy of Sciences, Borok, Russia) for organizing chemical analysis, Victoria V. Yurchenko (Papanin Institute for Biology of Inland Waters, Russian Academy of Sciences, Borok, Russia) for pH analysis. We also thank the anonymous reviewers, whose constructive comments helped to improve the paper.

Conflicts of Interest: The authors declare no conflict of interest.

Appendix A

Table A1. Abundances (raw counts) of oribatid mites in *Sphagnum* bog plots, Shichengskoe mire (*n*—number of samples).

Species [1]	Jul 2016, *n* = 48	Aug 2019, *n* = 53	Species	Jul 2016, *n* = 48	Aug 2019, *n* = 53
Achipteria coleoptrata (L., 1758)	2	22	*Limnozetes palmerae* Behan-Pelletier, 1989	642	474
Acrotritia ardua (Koch, 1841)	63	16	*Limnozetes rugosus* (Sellnick, 1923)	333	46
Adoristes ovatus (Koch, 1839)	12	18	*Liochthonius alpestris* (Forsslund, 1958)	94	334
Atropacarus striculus (Koch, 1835)	273	87	*Malaconothrus foveolatus* (Willmann, 1931)	–	688
Autogneta traegardhi Forsslund, 1947	1	–	*Malaconothrus monodactylus* (Michael, 1888)	259	333
Banksinoma lanceolata (Michael, 1885)	–	4	*Malaconothrus vietsi (Willmann, 1925)*	27	–
Camisia solhoeyi Colloff, 1993	3	–	*Microppia minus* (Paoli, 1908)	–	1
Carabodes labyrinthicus (Michael, 1879)	57	–	*Nanhermannia comitalis* Berlese, 1916	74	–
Carabodes rugosior Berlese, 1916	11	–	*Nanhermannia coronata* Berlese, 1913	421	182
Cepheus cepheiformis (Nicolet, 1855)	15	–	*Nothrus pratensis* Sellnick, 1928	222	236
Ceratoppia bipilis (Hermann, 1804)	1	–	*Oppiella nova* (Oudemans, 1902)	1446	436
Ceratoppia quadridentata (Haller, 1882)	2	–	*Oribatula tibialis* (Nicolet, 1855)	2	–
Ceratozetes sellnicki Rajski, 1958	–	1	*Parachipteria punctata* (Nicolet, 1855)	43	–
Chamobates cuspidatus (Michael, 1884)	24	–	*Pergalumna emarginata* (Banks, 1895)	12	22
Diapterobates humeralis (Hermann, 1804)	22	9	*Phthiracarus boresetosus* Jacot, 1930	184	14
Epidamaeus kamaensis (Sellnick, 1926)	1	–	*Phthiracarus laevigatus* (Koch, 1841)	4	–
Eupelops occultus (Koch, 1835)	24	–	*Pilogalumna tenuiclava* (Berlese, 1908)	48	32
Eupelops strenzkei (Knülle, 1954)	16	13	*Punctoribates sellnicki* Willmann, 1928	–	13
Fuscozetes fuscipes (Koch, 1844)	5	–	*Quadroppia quadricarinata* (Michael, 1885)	4	–
Fuscozetes setosus (Koch, 1839)	–	5	*Rhinoppia hygrophila* (Mahunka, 1987)	–	29
Galumna lanceata (Oudemans, 1900)	20	–	*Scheloribates circumcarinatus* Weigmann & Miko, 1998	61	9
Galumna obvia (Berlese, 1914)	17	–	*Scheloribates labyrinthicus* Jeleva, 1962	–	11
Heminothrus longisetosus (Willmann, 1925)	3	–	*Scheloribates laevigatus* (C.L. Koch, 1835)	176	3
Heminothrus peltifer (Koch, 1839)	43	1	*Suctobelbella palustris* (Forsslund, 1953)	141	17
Heminothrus thori (Berlese, 1904)	1	–	*Tectocepheus velatus* (Michael, 1880)	560	44
Hoplophthiracarus illinoisensis (Ewing, 1909)	796	949	*Trhypochthoniellus longisetus* (Berlese, 1904)	217	7
Hydrozetes lacustris (Michael, 1882)	38	15	*Trhypochthonius tectorum* (Berlese, 1896)	24	6
Hypochthonius rufulus Koch, 1835	90	1	*Trimalaconothrus foveolatus* Willmann, 1931	352	–
Liebstadia similis (Michael, 1888)	3	3	*Tyrphonothrus angulatus* (Willmann, 1931)	5	47
Limnozetes ciliatus (Schrank, 1803)	354	851	*Tyrphonothrus maior* (Berlese, 1910)	800	82
			Oribatida total	8048	5083

[1] Identification keys: Weigmann [66]; Balogh and Balogh [67]; Norton and Behan-Pelletier [68].

Table A2. Abundances (raw counts) of mesostigmatid mites in *Sphagnum* bog plots, Shichengskoe mire (*n* = 53).

Species [1]	August 2019
Lysigamasus lapponicus (Trägårdh, 1910)	21
Veigaia transisale (Oudemans, 1902)	25
Veigaia nemorensis (C.L.Koch, 1839)	11
Cheiroseius bryophilus Karg, 1969	13
Cheiroseius mutilus (Berlese, 1916)	9
Cheiroseius serratus (Halbert, 1915)	2
Cheiroseius laelaptoides (Berlese, 1887)	5
Platyseius italicus (Berlese, 1905)	8
Ololaelaps venetus (Berlese 1903)	12
Gaeolaelaps nolli (Karg, 1962)	4
Parazecon radiatus (Berlese, 1910)	54
Zercon zelawaiensis Sellnick, 1944	32
Prozecon kochi Sellnick, 1943	77
Epicrius bureschi Balogh, 1958	2
Acugamasus montanus (Willmann, 1936)	7
Mesostigmata total	282

[1] Identification keys: Karg [69]; Gilyarov and Bregetova [70]; Evans and Hyatt [71]; Evans and Till [72]; Mašán and Fend'a [73].

References

1. Rydin, H.; Jeglum, J.K. *The Biology of Peatlands*, 2nd ed.; Oxford University Press: Oxford, UK, 2013.
2. Gorham, E. Northern peatlands: Role in the carbon cycle and probable responses to climate warming. *Ecol. Appl.* **1991**, *1*, 182–195. [CrossRef] [PubMed]

3. Limpens, J.; Berendse, F.; Blodau, C.; Canadell, J.G.; Freeman, C.; Holden, J.; Roulet, N.; Rydin, H.; Schaepman-Strub, G. Peatlands and the carbon cycle: From local processes to global implications—A synthesis. *Biogeosciences* **2008**, *5*, 1475–1491. [CrossRef]
4. Kimmel, K.; Mander, Ü. Ecosystem services of peatlands: Implications for restoration. *Prog. Phys. Geogr.* **2010**, *34*, 491–514. [CrossRef]
5. Waddington, J.M.; Griffis, T.J.; Rouse, W.R. Northern Canadian wetlands: Net ecosystem CO_2 exchange and climate change. *Clim. Change* **1998**, *40*, 267–275. [CrossRef]
6. Bubier, J.L.; Moore, T.R.; Bledzki, L.A. Effects of nutrient addition on vegetation and carbon cycling in an ombrotrophic bog. *Glob. Change Biol.* **2007**, *13*, 1168–1186. [CrossRef]
7. Strack, M.; Waddington, J.M. Response of peatland carbon dioxide and methane fluxes to a water table drawdown experiment. *Global Biogeochem. Cycles* **2007**, *21*, GB1007. [CrossRef]
8. Camill, P.; Barry, A.; Williams, E.; Andreassi, C.; Limmer, J.; Solick, D. Climate-vegetation-fire interactions and their impact on long-term carbon dynamics in a boreal peatland landscape in northern Manitoba, Canada. *J. Geophys. Res. Biogeosci.* **2009**, *114*, G04017. [CrossRef]
9. Harris, A.; Charnock, R.; Lucas, R.M. Hyperspectral remote sensing of peatland floristic gradients. *Remote Sens. Environ.* **2015**, *162*, 99–111. [CrossRef]
10. McPartland, M.Y.; Kane, E.S.; Falkowski, M.J.; Kolka, R.; Turetsky, M.R.; Palik, B.; Montgomery, R.A. The response of boreal peatland community composition and NDVI to hydrologic change, warming, and elevated carbon dioxide. *Glob. Change Biol.* **2019**, *25*, 93–107. [CrossRef]
11. Tian, J.; Branfireun, B.A.; Lindo, Z. Global change alters peatland carbon cycling through plant biomass allocation. *Plant Soil* **2020**, *455*, 53–64. [CrossRef]
12. Tahvanainen, T. Water chemistry of mires in relation to the poor-rich vegetation gradient and contrasting geochemical zones of the north-eastern fennoscandian Shield. *Folia Geobot.* **2004**, *39*, 353–369. [CrossRef]
13. Wheeler, B.D.; Proctor, M.C.F. Ecological gradients, subdivisions and terminology of north-west European mires. *J. Ecol.* **2000**, *88*, 187–203. [CrossRef]
14. Bragazza, L.; Gerdol, R. Are nutrient availability and acidity-alkalinity gradients related in *Sphagnum*-dominated peatlands? *J. Veg. Sci.* **2002**, *13*, 473–482. [CrossRef]
15. Ruuhijärvi, R.; Lindholm, T. Ecological gradients as the basis of Finnish mire site type system. In *Finland—Land of Mires*; Lindholm, T., Heikkilä, R., Eds.; The Finnish Environment 23/2006; Finnish Environment Institute: Helsinki, Finland, 2006; pp. 119–126.
16. Hajkova, P.; Hajek, M. *Sphagnum* distribution patterns along environmental gradients in Bulgaria. *J. Bryol.* **2007**, *29*, 18–26. [CrossRef]
17. Markkula, I. Comparison of the communities of oribatids (*Acari*: *Cryptostigmata*) of virgin and forest ameliorated pine bogs. *Ann. Zool. Fenn.* **1986**, *23*, 33–38.
18. Borcard, D.; Von Ballmoos, V.C. Oribatid mites (*Acari*, *Oribatida*) of a primary peat bog pasture transition in the Swiss Jura Mountains. *Ecoscience* **1997**, *4*, 470–479. [CrossRef]
19. Starý, J. Contribution to the knowledge of the oribatid mite fauna (*Acari*, *Oribatida*) of peat bogs in Bohemian Forest. *Silva Gabreta* **2006**, *12*, 35–47.
20. Gergócs, V.; Hufnagel, L. Application of oribatid mites as indicators (review). *AEER* **2009**, *7*, 79–98. [CrossRef]
21. Gulvik, M.E. Mites (Acari) as indicators of soil biodiversity and land use monitoring: A review. *Pol. J. Ecol.* **2007**, *55*, 415–440.
22. Seniczak, A. Oribatid mites (*Acari*, *Oribatida*) and their seasonal dynamics in a floating bog mat in Jeziorka Kozie Reserve, Tuchola Forest (Poland). *Biol. Lett.* **2011**, *48*, 3–11. [CrossRef]
23. Lehmitz, R. The oribatid mite community of a German peatland in 1987 and 2012—Effects of anthropogenic desiccation and afforestation. *Soil Org.* **2014**, *86*, 131–145.
24. Minor, M.A.; Ermilov, S.G.; Philippov, D.A.; Prokin, A.A. Relative importance of local habitat complexity and regional factors for assemblages of oribatid mites (*Acari*: *Oribatida*) in *Sphagnum* peat bogs. *Exp. Appl. Acarol.* **2016**, *70*, 275–286. [CrossRef] [PubMed]
25. Minor, M.A.; Ermilov, S.G.; Philippov, D.A. Hydrology-driven environmental variability determines abiotic characteristics and Oribatida diversity patterns in a *Sphagnum* peatland system. *Exp. Appl. Acarol.* **2019**, *77*, 43–58. [CrossRef] [PubMed]
26. Donaldson, G.M. Oribatida (*Acari*) associated with three species of *Sphagnum* at Spruce Hole Bog, New Hampshire, US. *Can. J. Zool.* **1996**, *74*, 1713–1720. [CrossRef]
27. Kreyling, J.; Tanneberger, F.; Jansen, F.; van der Linden, S.; Aggenbach, C.; Blüml, V.; Jurasinski, G. Rewetting does not return drained fen peatlands to their old selves. *Nat. Comm.* **2021**, *12*, 5693. [CrossRef]
28. Crichton, K.A.; Anderson, K.; Bennie, J.J.; Milton, E.J. Characterizing peatland carbon balance estimates using freely available Landsat ETM+ data. *Ecohydrology* **2015**, *8*, 493–503. [CrossRef]
29. Harris, A.; Bryant, R.G. A multi-scale remote sensing approach for monitoring northern peatland hydrology: Present possibilities and future challenges. *J. Environ. Manag.* **2009**, *90*, 2178–2188. [CrossRef]
30. Dissanska, M.; Bernier, M.; Payette, S. Object-based classification of very high resolution panchromatic images for evaluating recent change in the structure of patterned peatlands. *Can. J. Remote Sens.* **2009**, *35*, 189–215. [CrossRef]
31. Anderson, K.; Bennie, J.J.; Milton, E.J.; Hughes, P.D.M.; Lindsay, R.; Meade, R. Combining LiDAR and IKONOS data for eco-hydrological classification of an ombrotrophic bog. *J. Environ. Qual.* **2010**, *39*, 260–273. [CrossRef]

32. Meingast, K.M.; Falkowski, M.J.; Kane, E.S.; Potvin, L.R.; Benscoter, B.W.; Smith, A.M.S.; Bourgeau-Chavez, L.L.; Miller, M.E. Spectral detection of near-surface moisture content and water-table position in northern peatland ecosystems. *Remote Sens. Environ.* **2014**, *152*, 536–546. [CrossRef]
33. Middleton, M.; Närhi, P.; Arkimaa, H.; Hyvönen, E.; Kuosmanen, V.; Treitz, P.; Sutinen, R. Ordination and hyperspectral remote sensing approach to classify peatland biotopes along soil moisture and fertility gradients. *Remote Sens. Environ.* **2012**, *124*, 596–609. [CrossRef]
34. Linkosalmi, M.; Tuovinen, J.P.; Nevalainen, O.; Peltoniemi, M.; Taniş, C.M.; Arslan, A.N.; Aurela, M. Tracking vegetation phenology of pristine northern boreal peatlands by combining digital photography with CO_2 flux and remote sensing data. *Biogeosciences* **2022**, *19*, 4747–4765. [CrossRef]
35. Pettorelli, N.; Vik, J.O.; Mysterud, A.; Gaillard, J.M.; Tucker, C.J.; Stenseth, N.C. Using the satellite-derived NDVI to assess ecological responses to environmental change. *Trends Ecol. Evol.* **2005**, *20*, 503–510. [CrossRef]
36. Boelman, N.T.; Stieglitz, M.; Rueth, H.M.; Sommerkorn, M.; Griffin, K.L.; Shaver, G.R.; Gamon, J.A. Response of NDVI, biomass, and ecosystem gas exchange to long-term warming and fertilization in wet sedge tundra. *Oecologia* **2003**, *135*, 414–421. [CrossRef]
37. Sonnentag, O.; Chen, J.M.; Roberts, D.A.; Talbot, J.; Halligan, K.; Govind, A. Mapping tree and shrub leaf area indices in an ombrotrophic peatland through multiple end member spectral unmixing. *Int. J. Remote Sens.* **2007**, *109*, 342–360.
38. Dube, T.; Pandit, S.; Shoko, C.; Ramoelo, A.; Mazvimavi, D.; Dalu, T. Numerical assessments of leaf area index in tropical savanna rangelands, South Africa using Landsat 8 OLI derived metrics and in-situ measurements. *Remote Sens.* **2019**, *11*, 829. [CrossRef]
39. Räsänen, A.; Juutinen, S.; Kalacska, M.; Aurela, M.; Heikkinen, P.; Mäenpää, K.; Virtanen, T. Peatland leaf-area index and biomass estimation with ultra-high resolution remote sensing. *GIScience Remote Sens.* **2020**, *57*, 943–964. [CrossRef]
40. Philippov, D.A.; Ermilov, S.G.; Zaytseva, V.L.; Pestov, S.V.; Kuzmin, E.A.; Shabalina, J.N.; Sazhnev, A.S.; Ivicheva, K.N.; Sterlyagova, I.N.; Leonov, M.M.; et al. Biodiversity of a boreal mire, including its hydrographic network (Shichengskoe mire, north-western Russia). *Biodivers. Data J.* **2021**, *9*, e77615. [CrossRef]
41. Rydin, H.; Sjörs, H.; Löfroth, M. Mires. *Acta Phytogeogr. Suec.* **1999**, *84*, 91–112.
42. Eurola, S.; Huttunen, A. Mire plant species and their ecology in Finland. In *Finland—Land of Mires*; Lindholm, T., Heikkilä, R., Eds.; The Finnish Environment 23/2006; Finnish Environment Institute: Helsinki, Finland, 2006; pp. 127–144.
43. Weigmann, G.; Deichsel, R. Acari: Limnic Oribatida. In *Chelicerata: Araneae, Acari I. Susswasserfauna von Mitteleuropa*; Gerecke, R., Ed.; Elsevier Spektrum Akademischer Verlag: München, Germany, 2006; Volume 7.
44. Landsat 8 (L8) Data Users Handbook. Version 5.0, U.S. Geological Survey. 2019. Available online: https://www.usgs.gov/landsat-missions/landsat-8-data-users-handbook (accessed on 20 May 2022).
45. Meyer, G.E.; Neto, J.C. Verification of color vegetation indices for automated crop imaging applications. *Comput. Electron. Agric.* **2008**, *63*, 282–293. [CrossRef]
46. Liu, Z.; Hu, H.; Yu, H.; Yang, X.; Yang, H.; Ruan, C.; Wang, Y.; Tang, J. Relationship between leaf physiologic traits and canopy color indices during the leaf expansion period in an oak forest. *Ecosphere* **2015**, *6*, 259. [CrossRef]
47. Gao, B.-C. NDWI—A normalized difference water index for remote sensing of vegetation liquid water from space. *Remote Sens. Environ.* **1996**, *58*, 257–266. [CrossRef]
48. Ceccato, P.; Flasse, S.; Tarantola, S.; Jacquemoud, S.; Grégoire, J.M. Detecting vegetation leaf water content using reflectance in the optical domain. *Remote Sens. Environ.* **2001**, *77*, 22–33. [CrossRef]
49. Rock, B.N.; Vogelmann, J.E.; Williams, D.L.; Vogelmann, A.F.; Hoshizaki, T. Remote detection of forest damage. *Bioscience* **1986**, *36*, 439–445. [CrossRef]
50. Welikhe, P.; Quansah, J.E.; Fall, S.; Elhenney, W.M. Estimation of soil moisture percentage using LANDSAT-based Moisture Stress Index. *J. Remote Sens. GIS* **2017**, *6*, 200. [CrossRef]
51. Genuer, R.; Poggi, J.-M.; Tuleau-Malot, C. Variable selection using Random Forests. *Pattern Recognit. Lett.* **2010**, *31*, 2225–2236. [CrossRef]
52. Murphy, M.A.; Evans, J.S.; Storfer, A.S. Quantifying *Bufo boreas* connectivity in Yellowstone National Park with landscape genetics. *Ecology* **2010**, *91*, 252–261. [CrossRef]
53. Chust, G.; Lek, S.; Deharveng, L.; Ventura, D.; Ducrot, D.; Pretus, J. The effects of the landscape pattern on arthropod assemblages: An analysis of scale-dependence using satellite data. *Belg. J. Entomol.* **2000**, *2*, 99–110.
54. Hamilton, S.K.; Kellndorfer, J.; Lehner, B.; Tobler, M. Remote sensing of floodplain geomorphology as a surrogate for biodiversity in a tropical river system (Madre de Dios, Peru). *Geomorphology* **2007**, *89*, 23–38. [CrossRef]
55. Madonsela, S.; Cho, M.A.; Ramoelo, A.; Mutanga, O. Remote sensing of species diversity using Landsat 8 spectral variables. *ISPRS J. Photogramm. Remote Sens.* **2017**, *133*, 116–127. [CrossRef]
56. Rocchini, D.; Boyd, D.S.; Féret, J.B.; Foody, G.M.; He, K.S.; Lausch, A.; Pettorelli, N. Satellite remote sensing to monitor species diversity: Potential and pitfalls. *Remote Sens. Ecol. Conserv.* **2016**, *2*, 25–36. [CrossRef]
57. Chust, G.; Pretus, J.L.; Ducrot, D.; Bedos, A.; Deharveng, L. Response of soil fauna to landscape heterogeneity: Determining optimal scales for biodiversity modeling. *Conserv. Biol.* **2003**, *17*, 1712–1723. [CrossRef]
58. Fleri, J.R.; Arcese, P. Predictive mapping to identify refuges for plant communities threatened by earthworm invasion. *Ecol. Solut. Evid.* **2021**, *2*, e12064. [CrossRef]
59. Skidmore, A.K.; Siegenthaler, A.; Wang, T.; Darvishzadeh, R.; Zhu, X.; Chariton, A.; De Groot, G.A. Mapping the relative abundance of soil microbiome biodiversity from eDNA and remote sensing. *Sci. Remote Sens.* **2022**, *6*, 100065. [CrossRef]

60. Bubier, J.L.; Rock, B.N.; Crill, P.M. Spectral reflectance measurements of boreal wetland and forest mosses. *J. Geophys. Res. Atmos.* **1997**, *102*, 29483–29494. [CrossRef]
61. Whiting, G.J. CO_2 exchange in the Hudson-Bay lowlands—Community characteristics and multispectral reflectance properties. *J. Geophys. Res. Atmos.* **1994**, *99*, 1519–1528. [CrossRef]
62. Zhang, W.; Lu, Q.; Song, K.; Qin, G.; Wang, Y.; Wang, X.; Li, H.; Li, J.; Liu, G.; Li, H. Remotely Sensing the Ecological Influences of Ditches in Zoige Peatland, Eastern Tibetan Plateau. *Int. J. Remote Sens.* **2014**, *35*, 5186–5197. [CrossRef]
63. Hasan, A.; Pilesjö, P.; Persson, A. On generating digital elevation models from liDAR data–resolution versus accuracy and topographic wetness index indices in northern peatlands. *Geod. Cartogr.* **2012**, *38*, 57–69. [CrossRef]
64. Carless, D.; Luscombe, D.J.; Gatis, N.; Anderson, K.; Brazier, R.E. Mapping landscape-scale peatland degradation using airborne lidar and multispectral data. *Landsc. Ecol.* **2019**, *34*, 1329–1345. [CrossRef]
65. Lees, K.J.; Artz, R.R.E.; Chandler, D.; Aspinall, T.; Boulton, C.A.; Buxton, J.; Cowie, N.R.; Lenton, T.M. Using remote sensing to assess peatland resilience by estimating soil surface moisture and drought recovery. *Sci. Total Environ.* **2021**, *761*, 143312. [CrossRef]
66. Weigmann, G. *Hornmilben (Oribatida)*; Die Tierwelt Deutschlands Bd. 76, Goecke and Evers: Keltern, Germany, 2006; p. 520.
67. Balogh, J.; Balogh, P. *Identification Keys to the Oribatid Mites of the Extra-Holarctic Regions*; Well-Press Publ Limited: Miskolc, Hungary, 2002; Volume 1, p. 453.
68. Norton, R.A.; Behan-Pelletier, V.M. Chapter 15. Oribatida. In *A Manual of Acarology*; Krantz, G.W., Walter, D.E., Eds.; Texas Tech Univ Press: Lubbock, TX, USA, 2009; pp. 430–564.
69. Karg, W. *Acari (Acarina), Milben. Parasitiformes (Anactinochaeta). Cohors Gamasina Leach: Raubmilben*, 2nd ed.; VEB Gustav Fischer Verlag: Jena, Germany, 1993; p. 523.
70. Gilyarov, M.S.; Bregetova, N.G. *Key to the Soil Inhabiting Mites, Mesostigmata*; Nauka: Leningrad, Russia, 1977; p. 717. (In Russian)
71. Evans, G.O.; Hyatt, K.H. A revision of the Platyseiinae (Mesostigmata: Aceosejidae) based on material in the collections of the British Museum (Natural History). *Bull. Brit. Mus. Nat. Hist. Zool.* **1960**, *6*, 27–101.
72. Evans, G.O.; Till, W.M. Studies on the British Dermanyssidae (Acari: Mesostigmata). Part II. Classification. *Bull. Brit. Mus. Nat. Hist. Zool.* **1966**, *14*, 107–370.
73. Mašán, P.; Fend'a, P. *Zerconid mites of Slovakia (Acari, Mesostigmata, Zerconidae)*; Institute of Zoology, Slovak Academy of Sciences: Bratislava, Slovakia, 2004; p. 238.